Nonlinear Structural Analysis Methodology and Dynamics Scaling of Inflatable Parabolic Reflector Antenna Concepts

Tham Sreekantamurthy[*]
Swales Aerospace, Hampton, Virginia, 23681, USA

James L. Gaspar.[†]
NASA Langley Research Center, Hampton, Virginia, 23681, USA

Troy Mann[‡] and Vaughn Behun[§]
Swales Aerospace

James C. Pearson, Jr [**]
SRS Technologies, Huntsville, Alabama 35806, USA

Stephen Scarborough[††]
ILC Dover, Frederica, Delaware 19946, USA

Ultra-light weight and ultra-thin membrane inflatable antenna concepts are fast evolving to become the state-of-the-art antenna concepts for deep-space applications. NASA Langley Research Center has been involved in the structural dynamics research on antenna structures. One of the goals of the research is to develop structural analysis methodology for prediction of the static and dynamic response characteristics of the inflatable antenna concepts. This research is focused on the computational studies to use nonlinear large deformation finite element analysis to characterize the ultra-thin membrane responses of the antennas. Recently, structural analyses have been performed on a few parabolic reflector antennas of varying size and shape, which are referred in the paper as 0.3 meters subscale, 2 meters half-scale, and 4 meters full-scale antenna. The various aspects studied included nonlinear analysis methodology and solution techniques, ways to speed convergence in iterative methods, the sensitivities of responses with respect to structural loads, such as inflation pressure, gravity, and pretension loads in the ground and in-space conditions, and the ultra-thin membrane wrinkling characteristics. Several such intrinsic aspects studied have provided valuable insight into evaluation of structural characteristics of such antennas. While analyzing these structural characteristics, a quick study was also made to assess the applicability of dynamics scaling of the half-scale antenna. This paper presents the details of the nonlinear structural analysis results, and discusses the insight gained from the studies on the various intrinsic aspects of the analysis methodology. The predicted reflector surface characteristics of the three inflatable ultra-thin membrane parabolic reflector antenna concepts are presented as easily observable displacement fringe patterns with associated maximum values, and normal mode shapes and associated frequencies. Wrinkling patterns are presented to show how surface wrinkle progress with increasing tension loads. Antenna reflector surface accuracies were found to be very much dependent on the type and size of the antenna, the reflector surface curvature, reflector membrane supports in terms of spacing of catenaries, as well as the amount of applied load.

---

[*] Aerospace Engineer, M.S. 230, Swales Aerospace, Hampton, Virginia, AIAA Member.
[†] Aerospace Engineer, M.S. 230, NASA Langley Research Center, Hampton, Virginia, AIAA Member.
[‡] Aerospace Engineer, M.S. 230, Swales Aerospace, Hampton, Virginia, AIAA Member.
[§] Aerospace Engineer, M.S. 230, Swales Aerospace, Hampton, Virginia, AIAA Member.
[**] Aerospace Engineer, SRS Technologies, Huntsville, Alabama, AIAA Member
[††] R&D Engineer, ILC Dover, Frederica, Delaware, AIAA Senior Member

I. Introduction

The antenna reflector surface shape accuracy is an important factor affecting the electromagnetic performance of the antennas. Evolving newer classes of large ultra-thin membrane inflatable and deployable antenna structures are inherently very flexible, and hence susceptible to shape distortions in the space operating environment. The shape accuracy is defined as the degree to which the actual shape of the structure deviates from the intended shape (Ref. 1). Therefore, reflector surface accuracy has been the primary focus in the analysis and design of antennas (Ref. 2-3). A variety of parabolic reflectors antenna configurations of lower weight have been developed based on advanced structural concepts utilizing composite materials, and thin membrane shell structures (Ref. 4-5), and some of the recent developments are discussed in References 6 through 9. New critical design requirements (Ref. 10-11), addressing structural flexibility, control-structure interactions, thermal and operational load requirements have resulted in additional challenges for the analysis, design and fabrication of antennas. The structural analysis plays an important role in the evaluation of antenna reflector deformation characteristics to assess the reflector shape distortions under a variety of such loadings. Analytical reflector surface accuracy predications become crucial when ground testing of large flexible antennas is impossible due to inherent difficultly in testing of antennas to simulate the extremely low structural loading associated with the zero-gravity condition of space. In particular, nonlinear finite element analysis is essential (Ref. 12) to tackle the challenges of complex loading patterns and boundary conditions that are typical of an asymmetric inflatable membrane antenna with an off-axis parabolic reflector supported on a torus ring via catenary attachments. An overview of the recently initiated inflatable antenna program at Langley and at Glenn Research Center has been presented in Reference 13. The reference describes the radio frequency tests, structural tests, and analysis conducted on a laboratory article of the antenna, and summarizes the structural and electromagnetic characteristics of the test article.

As part of the continued effort in the prediction of antenna reflector surface characteristics, new structural analyses were performed on subscale and full scale inflatable antennas. Three parabolic reflector antenna concepts of varying size and shape were considered, and these are a 0.3 meters subscale off-axis reflector, a 2 meters half-scale symmetric reflector with rigid central dish, and a 4 meters full-scale off-axis reflector inflatable dish antenna. The primary goal of these antenna analyses was to study and evaluate various nonlinear computational analysis techniques for predicting structural responses of antenna designs; and to computationally evaluate the reflector structural characteristics of three particular antenna designs for future correlation and validation with laboratory tests. Various aspects studied in the analysis technique evaluation included suitability of nonlinear analysis methodologies and solution techniques; ways to speed convergence in iterative methods; sensitivity of responses with respect to structural loads, such as inflation pressure, gravity, and pretension loads in the ground and in-space conditions; and approaches to ultra-thin membrane wrinkling characteristics. This paper discusses the structural analyses of the three antenna concepts, including development of the finite element models, the nonlinear static and normal mode response and their sensitivities with respect to structural loads, membrane wrinkling characteristics, and predicted structural response characteristics. In addition, some discussion on scaling of the 2 meter antenna and related computational results is also presented. Antenna reflector surface accuracies are shown to be very much dependent on the type and size of the antenna, the reflector surface curvature, reflector membrane supports in terms of spacing of catenaries, as well as the amount of applied load.

II. Description of the Inflatable Antennas

A laboratory article of a 0.3 meter subscale reflector inflatable dish antenna is shown in Figure 1. This laboratory article has been built to simulate an off-axis parabolic reflector dish antenna required to operate in the deep space network frequency range (Ref. 14). The reflector is made of ultra-thin membrane material of about 0.7 mil thickness. The reflector dish is inflated to a nominal internal pressure of 17 Pa and held stretched by a set of soft elastic catenaries in tension around the circumferential edge of the dish. Figure 2 shows the geometrical construction of an off-axis parabolic surface sliced from a parabolic surface of revolution to form the reflector of the antenna. A mirror image of this sliced surface was used as a canopy surface and is bonded at the periphery to form two parabolic shell segments of the inflatable dish.

Figure 1. 0.3 meter reflector antenna dish mounted on a frame.

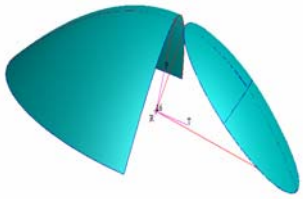

Figure 2: Geometrical Surface of off-axis Parabolic reflector

Figure 3. 4x6 meter full scale parabolic reflector antenna.

A full-scale 4x6 meter off-axis parabolic reflector antenna (Ref. 14-16) is shown in Figure 3. This reflector has a different geometry than the 0.3 meter reflector described above, in terms of the angle subtended by the plane that slices the parabolic surface. Here, the film material is about 0.8 mil thick, the membrane dish is inflated to a nominal pressure of 10 Pa, and it is stretched by 200 hundred catenaries at the periphery. The figure also shows an inflated torus structure, which is not considered in the structural model of the antenna.

A 2 meter half-scale hybrid inflatable antenna (Ref. 17) is shown in Figure 4. This reflector antenna has a symmetric parabolic shape and is different from the above off-axis reflectors. Also, this reflector has a central annular region for housing a rigid reflector. The antenna dish is comprised of two outer layers of inflatable membranes, which are held to a parabolic shape via inflation internal pressure and an additional un-inflated middle layer to take tension loads from the surrounding catenaries around the edge of the dish (Fig. 5). The antenna dish is made of a thicker composite layer underneath these other layers of inflatable membranes.

Figure 4: 2 meter half-scale Hybrid Inflatable Antenna

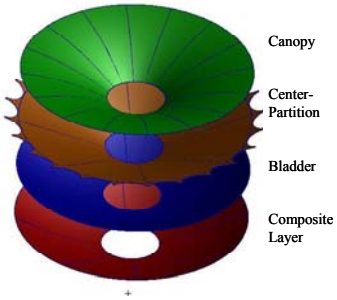

Figure 5: Layers in the Hybrid Inflatable Antenna.

III. Analysis Methodologies, Solution Techniques Investigated

Practical application of the nonlinear structural analysis to the types of antennas described above was a challenging experience in itself, because of the many intricate details surrounding each application. A variety of computational studies were conducted while addressing the antenna structural analysis problem, which included studies into nonlinear analysis techniques, iterative solution methods, availability of techniques in commercial codes such as NASTRAN and ABAQUS, wrinkling of thin membranes and sensitivities of structural response to internal pressure, gravity, and tension loads. This section presents theoretical background and insights gained for each of the methodologies investigated; numerical results for each of the three antennas studied are presented later in this paper.

A. Nonlinear Analysis Techniques

The structural analysis problem of an ultra-thin membrane antenna structure is a nonlinear large displacement problem, wherein a membrane undergoes a large motion under the action of in-plane tension loads and lateral pressure loads. The nonlinear finite element analysis approach is based on an iterative strategy that involves finding a net balanced set of forces among externally applied forces, constraint reaction forces at membrane support, and internal nodal forces in the membrane. Often, the basic mechanism of the membrane structure carrying external loads would be destroyed if the internal forces are not completely balanced with pure tension forces, if these forces are not balanced, the membrane experiences internal compression and/or shear loads in the membrane, which the membrane cannot inherently carry causing it to buckle. Also, the basic assumption that a membrane structure is only capable of carrying tension load would be completely violated, if an unbalanced set of tensile forces exists at the boundary of the membrane. The way a membrane is actually supported in a real antenna, as fabrication techniques are evolving, may be far from the ideal roller support requirement for a membrane to take the support load in the plane of the membrane.

The equilibrium equation in terms of forces can be expressed as $\{P\} + \{Q\} - \{F\} = \{0\}$, where, $\{P\}$, $\{Q\}$ and $\{F\}$ represent external force, constraint force, and internal forces, respectively, which are unknown nonlinear functions of displacement. The strategy involved in solving this equation consists of two steps, first, simplify this equation by replacing it with a first order linear equation by Taylor series expansion in terms of displacements, and then solve for unknown displacement $\{U\}$ with an initial guess, which is iteratively updated with newer set of linear solution of displacement until the equilibrium of forces are satisfied. Newton's method is applied to numerically solve a linear system of equations in terms of incremental set of displacement $\{\Delta U\}$ at the i^{th} iteration,

$$[K_t]\ \{\Delta U^i\} = \{R^{i-1}\}$$

where $[K_t]$ is the tangential stiffness matrix, which consists of the linear stiffness, stiffness due to large rotation, and geometrical stiffness (or differential stiffness) dependent on the $\{U^{i-1}\}$ and initial stress level; and $\{R^{i-1}\}$ is the unbalanced residual force set. After computing the incremental displacement at the i^{th} iteration, next challenge is to move forward with an appropriate step in n dimensional unknown displacement space to determine $\{U^{i+1}\} = \{U^i\} + \{\Delta U^i\}$, to seek a minimum value of residual unbalanced force. This process is highlighted below.

B. Iterative Solution Schemes

While the application of the iterative nonlinear analysis technique may seem straight forward, it has often lead to numerical convergence difficulties in solving the thin membrane problems. Thus, it became essential to dwell on the theoretical basis for finding an equilibrium set of forces to get some insight into overcoming convergence difficulties. A basis for this iterative solution scheme comes from an analogous solution to a nonlinear programming problem with an objective function in n dimensional displacement space. The total potential energy of the structure, when approximated as quadratic objective function of displacement, will have a minimum value at a solution point that minimizes the total potential energy. A feasible displacement vector $\{\Delta U^i\}$ sought in the iterative search must satisfy two conditions: a Hessian of stiffness matrix must be positive semi-definite, and the product $\{R\}\{\Delta U^i\} \geq 0$, where equality is satisfied at a solution point. A local minimum point in a particular feasible direction is obtained from the line-search for scaling parameter α from the equation in the vector direction $\{\Delta U^i\}$, such that $\{R^i\}\{\Delta U^i\} = 0$,

$$U^i = U^{i-1} + \alpha \, \Delta U^{i-1}$$

The iteration solution is continued until $\{\Delta U^i\}$, along with $\{R\}$ become negligible, which is signified by a suitable displacement, load or energy based convergence criteria.

Although, this iterative solution scheme has been known to provide a readily convergent solution in well posed nonlinear problems, such as beams and plates, it was found to be not so well behaved in the ultra-thin membrane antenna structural applications. The thin membrane structure can experience very large displacements or rotations under the application of a small incremental load, due to local buckling or wrinkling of the membrane. Such large incremental deformation results in negative factors in the decomposition of the updated stiffness matrix at the i^{th} iteration, causing premature termination of the computation. In the ultra-thin membrane problem, such large deformation at the incremental load step was visually observed by developing displacement plots, which often showed significant local deformations when plotted in an exaggerated scale. The problem was overcome by selecting only a small incremental load in that iteration. Further, the nature of internal loads plotted for that locally deformed area indicated that local area of membrane is nearly undergoing internal compression or shear loading at that intermediate iterative step. Such plots provided an insight into the wrinkling tendency of the membrane, which otherwise would be normally stable under uniform tension load. Also, it was found that redistribution of membrane loads by artificially introducing tension load in the membrane at an iterative step helped to overcome the convergence problem. A combination of structural behavior along with judicious selection of convergence tolerance parameters has helped to obtain a best possible solution in the ultra-thin membrane antenna structures.

C. Membrane Statics via Implicit and Explicit Dynamics Analysis

One of the main difficulties of the static solution scheme described above is the local wrinkling of the antenna membrane that causes a numerical instability that tends to hinder the static solution process. Another way to look at the highly flexible membrane problem is to model it as a dynamics problem. The inflatable membrane dish antenna static problem can also be viewed as a dynamics problem with time varying application of inflation pressure load, and tension load to simulate the transient response of a membrane, which is expected to settle down to its static position over a long period of time. The main idea behind applying an equivalent dynamic load is to supply a small amount of kinetic energy in addition to strain energy in the static structure to help the membrane overcome the typical local wrinkling or buckling that otherwise causes numerical convergence problems in the static solution process. The solution for the transient response is performed by an implicit analysis technique that involves decomposition of the stiffness matrix. Yet another way to model the antenna membrane problem is to apply quasi-static loads to simulate a slow inflation dynamics, and then solve the problem by an explicit analysis technique; this approach does not require stiffness matrix decomposition, and hence, the solution is expected to converge in a shorter time than the implicit analysis approach. How these implicit and explicit analysis techniques actually fared in the three membrane problems are discussed in subsequent sections of this paper.

D. MSC/NASTRAN and ABAQUS Solution Schemes for Antenna Membrane Responses

In this study, nonlinear analysis techniques available in two commercial codes MSC/NASTRAN and ABAQUS were employed to compute antenna membrane structural response characteristics under external loads.

1) Statics finite element computational analysis of the antenna structure was performed using the nonlinear structural analysis solution sequence 106 of the MSC/NASTRAN program (Ref. 18). This solution sequence 106 is based on the large displacement formulation. After finding the static displacement solution, the normal mode vibration analysis was performed using solution sequence 103 at the last converged iteration of the static analysis to determine the natural frequencies and mode shapes.

2) Statics and Dynamics finite element analysis techniques available in ABAQUS were also used in parallel with the above analysis (Ref. 19). In this paper, the ABAQUS/Standard Implicit analysis method, based on Newton-Raphson iterative procedure has been used for static analysis, and Implicit Dynamics analysis has been used for the equivalent dynamics problem. Also, ABAQUS Explicit analysis scheme has been applied on the antenna membrane problem.

E. Membrane Wrinkling Analysis

In situations where there is a significant deviation in an actual fabricated antenna reflector surface as compared to ideal standards of a membrane structure, an assessment of the actual load carrying capability of the membrane structure as well as the extent of surface wrinkling becomes an essential element in the antenna design process. In view of this, available analytical schemes (Ref. 20-22) and programs were applied to evaluate the antenna membrane wrinkling characteristics. The basic idea behind the wrinkle formulation comes from the fact that membrane can neither carry bending nor compressive load, and hence, when membrane stresses tend to zero, wrinkles appear over part or all of the membrane. These formulations are based on major and minor principal stresses in the membrane, and if both are greater than zero, then the membrane is taut; and if both are zero then the membrane is unloaded; and when one is zero and other is nonzero wrinkles form. Also, the principal strain formulation, and a combination of stress and strain formulations are available. Based on the principal stress-strain formulations, a constitutive equation can be developed for the wrinkled element, where stiffness matrix is appropriately chosen depending on the stress (σ) and strain (ε) state, and this matrix has the following form:

$$\sigma = D\,\varepsilon, \quad \text{where} \quad \sigma = (\sigma_x, \sigma_y, \sigma_{xy})^T, \ \text{and} \ \varepsilon = (\varepsilon_x, \varepsilon_y, \gamma_{xy})^T,$$

$$\text{where } D_{wrinkled} = E/4\begin{bmatrix} 2(1+P) & 0 & Q \\ & 2(1+P) & Q \\ Q & Q & 1 \end{bmatrix}, \quad D_{taut} = E/4\begin{bmatrix} 1 & \nu & 0 \\ \nu & 1 & 0 \\ 0 & 0 & (1-\nu)/2 \end{bmatrix}, \text{ and } D_{slack} = 0,$$

and where $P = (\varepsilon_x - \varepsilon_y)/(\varepsilon_1 - \varepsilon_2)$, and $Q = \gamma_{xy}/(\varepsilon_1 - \varepsilon_2)$, ν is the Poisson's ratio, E is the modulus of elasticity of the membrane.

To implement this formulation, the capabilities of ABAQUS program to add on user subroutines (Ref. 23) were used. The wrinkling pattern predicated for the 0.3 meter antenna using this approach is discussed later.

F. Dynamics Scaling of the Inflatable Membrane Antenna

Large size inflatable reflector antennas are envisioned for better electromagnetic performance of the antenna. The design of a large size antenna is dependent on accurate prediction of structural response characteristics, since laboratory testing of large antennas is not practical due to size, space, and load constraints. Structural characteristics of these large antennas are based on validated structural analyses of reduced scale antenna models that are correlated with data from laboratory size articles. Scaling function of inflatable antennas is derived in terms of several empirical relations such as relation between RMS surface errors in terms of the diameter of the reflector surface, as described in reference 24. The reference also discusses the sensitivity of focal length as a function of the inflation pressure, and modulus of the material. A plot of operating internal pressure verses reflector diameter is given in reference 25. Constant thickness scaling has been suggested in reference 26.

While evaluating the antenna characteristics, a quick attempt was made to estimate the characteristics of large scale models by simply scaling up the finite element models of the antennas. The structural analysis results from the large scale antenna were compared with the reduced scale model in terms of deformations, and natural frequency and mode shapes. Also, it is assumed that the thickness of membrane remains the same during scaling, and that the internal pressure scaled inversely by square of the antenna diameter. The scaling approach has been demonstrated on the 2 meter inflatable antenna and the results are discussed next section.

IV. Numerical Predications of Antenna Structural Characteristics

The salient structural characteristics of each of the three antennas (0.3 meter subscale, 2 meter half-scale, and 4 meter full scale) were evaluated using the previously discussed nonlinear techniques and are described here in terms of deformation shapes, normal modes, wrinkling characteristics, and sensitivities of the deformation with respect to pressure load, gravity and catenary pretension loads. The reflector surface deformation characteristics are plotted as displacement plots that show fringe pattern indicating various levels in magnitudes of displacements with respect to the original un-deformed surface of the reflector. Each of these plots will indicate a maximum level of displacement among the various fringe bands of displacements. Although a single RMS value has been commonly used to characterize surface deviation level in antenna electromagnetic computations, no additional calculations were made here to compute this quantity, since plotted fringe pattern along with a maximum value of the uniformly scaled color bands provide more information on the surface deviation characteristics than a single RMS value for evaluation of structural characteristics.

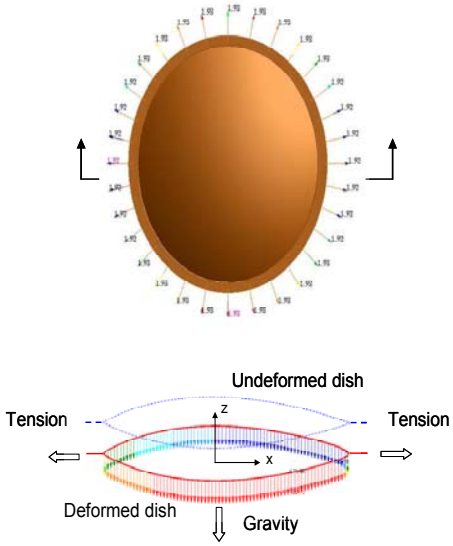

Figure 6: Antenna Dish of Elliptical Plan-form, and Applied Forces.

A. 0.3 meter Subscale Antenna

A finite element model was developed for the structural analysis of the 0.3 meter off-axis parabolic reflector membrane antenna described earlier (Figure 1). Figure 6 shows the elliptical plan form of the antenna dish surrounded with catenaries, each of which is rigidly fixed at one end. The figure also shows the cross-section of the inflated antenna dish, and the catenary tension, and gravity forces and the internal pressure are acting on the dish. The top and bottom membrane of the reflector dish are modeled with four-noded quadrilateral membrane elements. The outer strip of the reflector membrane, which is elliptical shaped ring, was modeled using quadrilateral shell elements. Catenaries were modeled with a set of beam elements with temperature dependent material properties, so that desired pre-stress loads in the catenaries can be generated by suitable selection of temperature loads. The finite element model has a total of 9752 elements and 9849 nodes. The reflector dish is inflated to an internal pressure load of 17 Pa, and also subjected to 1G gravity load. The cross-section of the reflector dish undergoes a non-uniform deformation under the action of the applied loads, and this non-uniformity of deformation is denoted by a set of vector lines of unequal length on the top and bottom surface of the dish, as plotted in Figure 6.

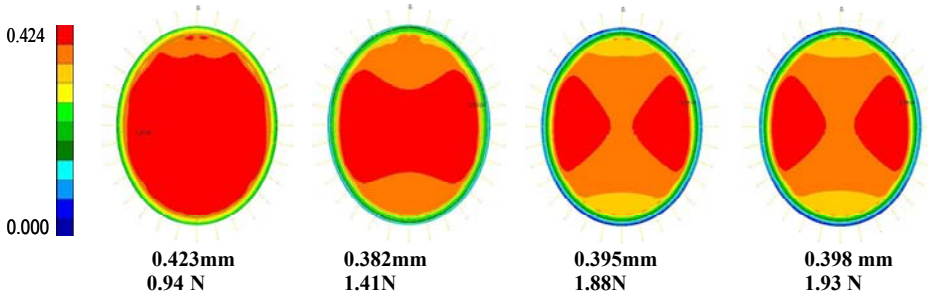

Figure 7: Reflector Surface Deformation Pattern and Catenary Tension.

The reflector surface deformation fringe pattern computed by NASTRAN Sol. 106 is plotted in the Figure 7, along with the maximum value of displacement for different catenary tensions. The deformation field shown in the first case, although nearly uniform, has maximum deformation because the dish is sagging under gravity field and the catenary tension force of 0.94 N is not enough to pull the dish up against the gravity field. The higher catenary force applied in the subsequent cases reduces this sag as the tension force gets reacted within the membrane, which is seen from the various fringe patterns in the figure. The indicated variation in deformation pattern is attributed to two factors: (1) uniform tension load applied around the elliptical plan form of the dish resolves into unequal net

distribution along major and minor axes of the ellipse, and (2) the non-uniform cross-section of the off-axis parabolic reflector dish, introduces unsymmetrical deformation. At higher tension loads, the membrane began to wrinkle (Figure 8) resulting in large rotations in MSC/NASTRAN runs that caused convergence problems. Alternate approaches were tried to avoid such problems by using artificial stiffness terms (KDIAG factor) to avoid negative values in the stiffness matrix to be decomposed. Use of such artificial factors resulted in local distortions in the membrane deformation. Also, the membrane wrinkles were also developing because the tension line force in the catenaries gets transferred as unwanted concentrated forces on the membrane elements at junction point of the outer strip and catenary. At higher tension loads, the computations did not converge. Figure 9 shows exaggerated scale plots of radial deformation pattern on the top and bottom surfaces of the reflector dish, with and without the gravity normal to the plane of dish. Notice that the top and bottom surface deformation is not symmetrical because of unsymmetrical net loading resulting from gravity force and internal pressure in the dish.

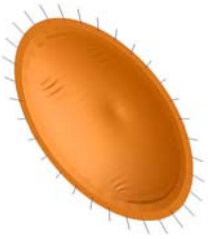

Figure 8: Membrane Wrinkling.

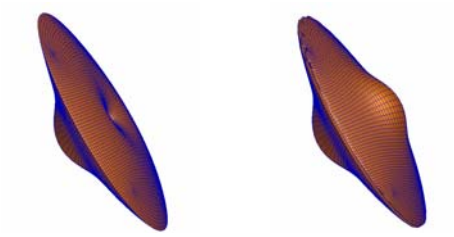

Figure 9: Deformation in 1g and 0g Gravity field.

Next, the static implicit nonlinear analysis technique available in ABAQUS/Standard was applied to the 0.3 meter antenna. Initial runs with the ABAQUS solution process, with combined application of pressure, gravity, and catenary pretension loads, ended up in taking enormous amount of computer time (days) as the step size got reduced to order of E-7 in the iterative process. The introduction of ABAQUS parameters called STABILIZE, and FACTOR to make the solution converge introduced unrealistic localized distortions in the membrane. This problem was overcome by changing of the order of application of the loads to apply the pressure load first, followed by uniformly distributed tension load of 0.2N/M around the edge. Here, it may be noted that uniformity of edge tension has been attained via application of tension load at each of the nodes on the outer edge, rather than by the application of catenary tension loads at sparsely spaced catenary attachment points, as was done before. The idea was to avoid the introduction of non-uniform tension loading in the membrane due to discrete loads from sparsely spaced catenaries. Gravity load was not applied in this case. The deformations computed under uniform pressure load alone are shown as plot (1) in Figure 10, which produces non-uniform surface deformation because of unsymmetrical reflector structure. Plot (2) in the figure shows deformation for the combined load case of uniform pressure and uniform tension. These results show that the non-uniform pattern in the displacement field of the inflated antenna in the zero-gravity condition can be smoothened out to a more desirable uniform circular displacement pattern, by the application of uniformly distributed tension load around the edge of the dish. Such a circular displacement pattern is difficult to attain in a reflector with a small number of catenaries, because sparse catenary spacing and associated point loads produce local membrane wrinkling, which in turn causes convergence problems in the solution process.

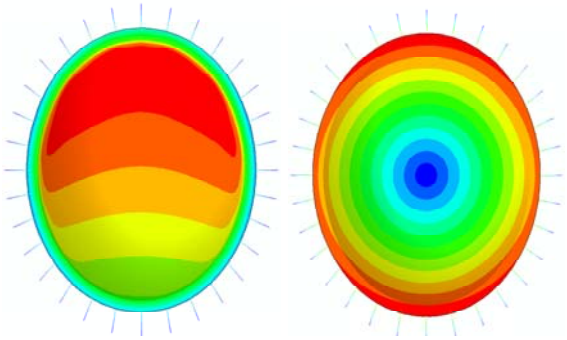

Figure 10: Deformation Due to (1) Pressure load only, (2) Pressure plus uniform tension around edge.

The ABAQUS static implicit analysis was also performed with catenary tension loads, along with 1g gravity load, and the displacement patterns for this case are plotted in Figure 11. The displacement values were slightly

lower than those obtained from NASTRAN run (Figure 7) because a higher catenary modulus was used here to make the runs converge. A higher catenary stiffness value allowed the catenaries bear more tension load, thereby artificially relieving the uneven point loads to be carried by the membrane to make it less prone to wrinkling, and hence temporarily avoided the usual convergence problem. It was found from these static implicit analyses that the membrane deformation patterns can be evaluated as described here; however, convergence to a solution is not assured for all combinations of load cases. Hence other alternatives were explored as described below.

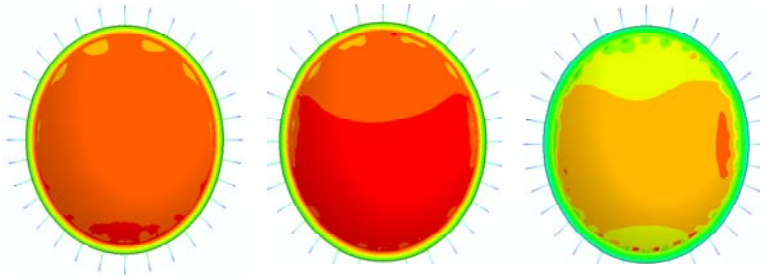

0.49 mm
0.47 N

0.34 mm
0.89 N

0.31mm
1.75N

Figure 11: Static Implicit solution on 0.3m Antenna.

The application of the dynamic implicit solution scheme in ABAQUS was explored on the 0.3 meter antenna for the 1g gravity case using a catenary tension of 0.9N. A plot of the time history of deformation, acceleration and velocity results at the center of reflector surface is shown in Figure 12. At the end of 5.0 seconds the velocity and accelerations settled to a zero value, indicating a static equilibrium condition. The idea in applying the dynamic load was to overcome the wrinkling tendency in the initial stages of loading, and then allow the dynamic load and the resulting dynamic displacement to settle into the static condition. Figure 13 shows the displacement pattern from this dynamic implicit run for the 0.9 N catenary tension load. The dynamic implicit solutions were accomplished without any convergence problems in all the three cases of tension load shown in the figure.

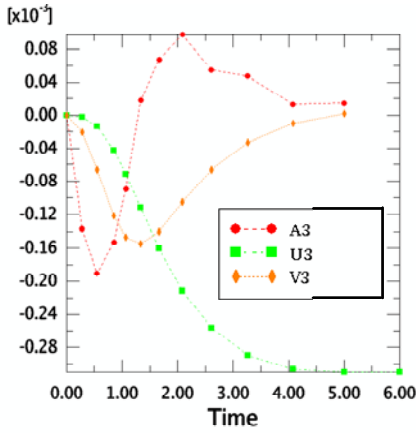

Figure 12: Time history of Displacement (U), Acceleration (A), and Velocity (V) at Center of reflector.

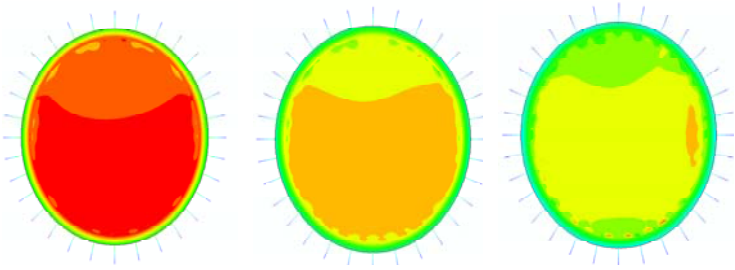

0.34 mm
0.89 N

0.29 mm
1.30 N

0.30 mm
1.70 N

Figure 13: Dynamic implicit Solution of 0.3 meter antenna.

Dynamic explicit analysis of 0.3 meter antenna was also performed using ABAQUS to simulate the quasi-static condition of inflation. Figure 14 show the time snap shot of antenna surface deformation as it goes through the inflation process. The steady static condition was checked by a plot of strain energy and kinetic energy in the system, wherein the kinetic energy becomes small at the end of prescribed inflation period.

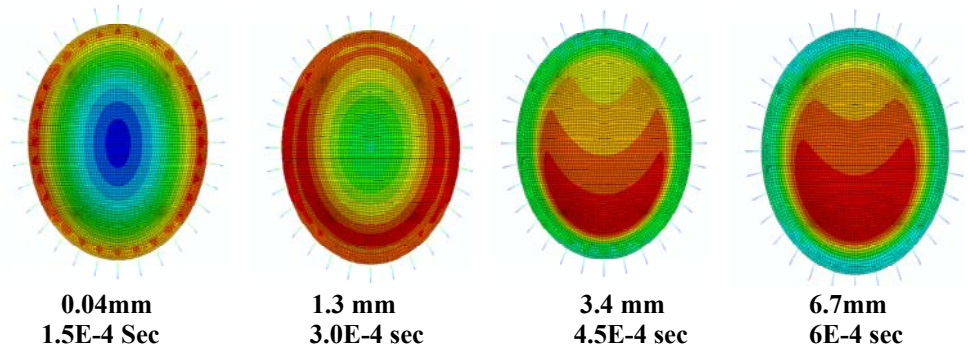

Figure 14: Snap shot of dish surface as it gets Inflated under pressure.

Finally, a wrinkle analysis was performed on the 0.3 meter antenna dish. Figure 15 shows the wrinkles on the surface of the reflector as a result of the various levels of tension load applied on the model. It can be seen from these plots that wrinkle begins at one of the catenary attachment points and progresses into the inner region of the surface as more tension load is applied. It is interesting to note that the wrinkle pattern predicted here resembles what was seen on the laboratory article of the antenna.

The details of the structural tests conducted on the laboratory article of the 0.3 m subscale antenna are described in reference 13. The reference describes and discusses the comparison of analytical results with measured data on the reflector deformations, natural frequencies and mode shapes

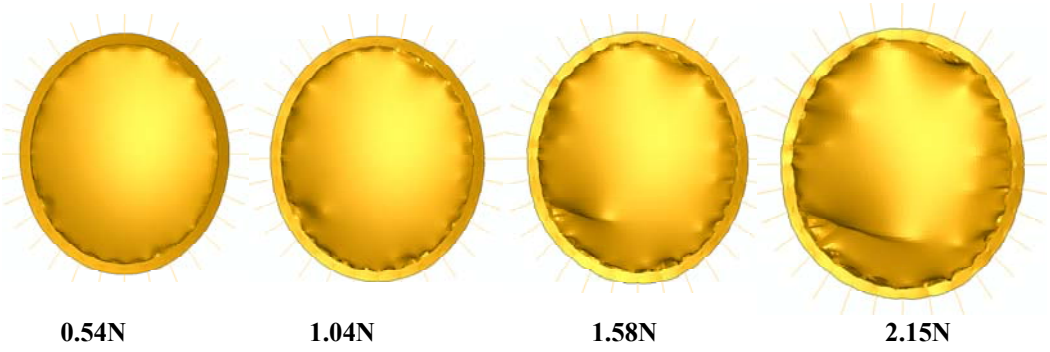

Figure 15: Wrinkling characteristics of the 0.3 meter antenna reflector.

B. 4x6 Meter Full Scale Antenna

The 4x6 meter full scale inflatable antenna (Figure 3) scales to about 15 times larger than that of the 0.3 meter antenna. However, the cross-section of the off-axis reflector surface does not symmetrically scale with that of the 0.3 meter antenna, since it has been designed to operate at a different electromagnetic operating range. The finite element model of the antenna is shown in Figure 16. There are 7800 quadrilateral membrane elements representing reflector membrane, 200 beam elements representing catenaries, and there are 8402 nodes in the model. The torus structure is not modeled. The structural characteristics of this 4x6 meter full scale antenna reflector were evaluated using ABAQUS implicit analysis program, since implicit analysis was found to work well on the 0.3 meter antenna. The reflector surface deformation results from this analysis for the loading conditions of internal pressure of 10Pa, gravity at 1G, and tension load of 1.24N are shown in Figure 17. The first plot is for the analysis case of internal pressure load only, and subsequent plots are for different loads added in sequence of internal pressure, gravity and pretension load. As pretension is applied the magnitude of deformation is reduced. It can be seen that this reflector has significant localized deformation at the top region of the reflector, as indicated by the red color fringe band. The deformation pattern of the 4x6 full scale model was seen to be significantly influenced by the steep curvature

associated with its off-axis orientation of the surface, while such pattern was not so dominant in the 0.3 meter reduced scale model. The natural frequency analysis was also performed at the nonlinear deformed configuration and some of basic normal modes are plotted in Figure 18.

C. 2 Meter Half-Scale Antenna

The structural analysis of the 2 meter half-scale inflatable antenna (see Figures 4 and 5) was performed using ABAQUS implicit analysis procedure. The finite element model developed for this antenna is shown in Figure 19(a). There are 25,218 elements of type quadrilateral and triangular membrane elements, and 23,216 nodes in this finite element model. The antenna is subjected to 60 Pa internal pressure, and 30 N catenary tension load, which is applied as a concentrated load tangential to the surface of the reflector. The reflector is supported at the outer rim of the rigid reflector, located at the centre of the dish, with all six degrees of freedom fixed at each of the support nodes. The loading is applied in sequences with pressure load first, followed by gravity load, and then finally the tension load is applied. The deformation results from the implicit analysis for the combined load are plotted in Figure 19 (b through d) for the different membrane layers of the antenna. The canopy is seen to undergo maximum amount of deformation compared to the other layers.

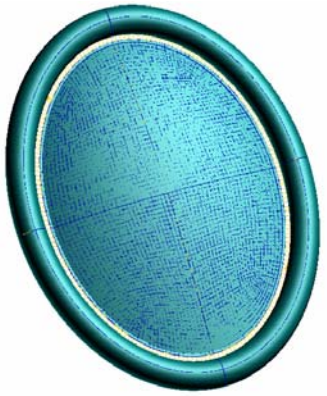

Figure 16: Finite Element Model of 4x6 meter Full Scale Antenna.

At the end of the nonlinear static implicit analysis iteration, an eigen-value analysis was performed on the deformed configuration of the antenna structure. The natural frequencies and mode shapes obtained from the analysis are plotted in Figure 20 for a few selected low frequency modes. These basic modes depict axis-symmetrical motion of the symmetric shell structure. The low frequency modes of the antenna are predominantly caused by the composite shell layer, since it is much stiffer and heavier than the canopy and other membrane layer. The mode shown at 70.3 Hz is caused by the joints (overlapping portion of the membrane) which are thicker than the membrane itself.

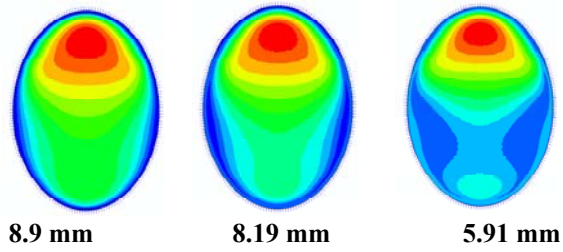

Figure 17: 4x6 meter reflector deformation under pressure, gravity and pretension load.

An experimental study on the structural dynamics of this 2 meter antenna has been described in Reference 27. A comparison of test and analysis has not been done at this time, but is a planned future work.

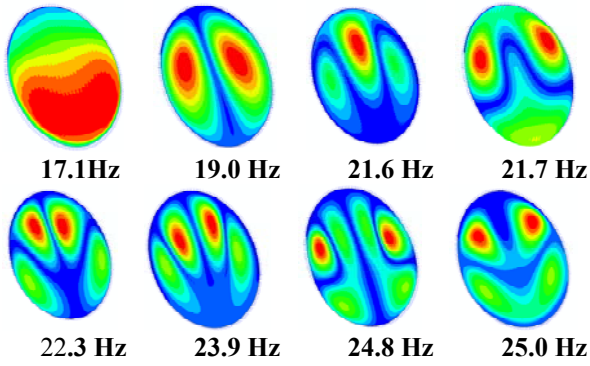

Figure 18: Natural Frequencies and Normal Modes of the 4x6 meter parabolic reflector antenna.

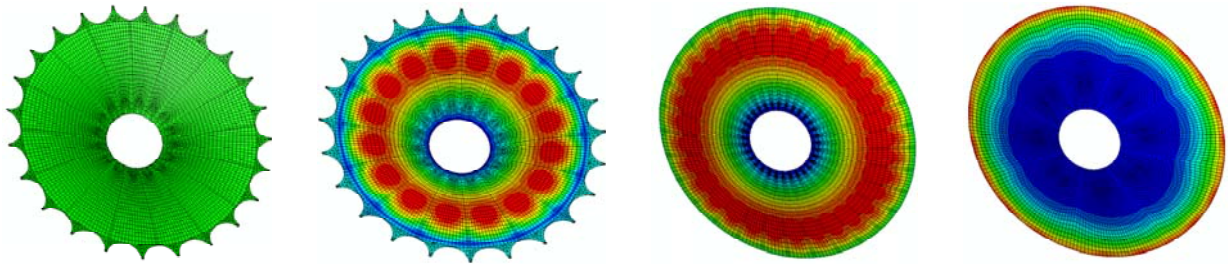

Figure 19: 2 meter half-scale inflatable antenna -- FEM model (a); and deformation patterns of the Canopy (b), bladder (c), and central partition (d).

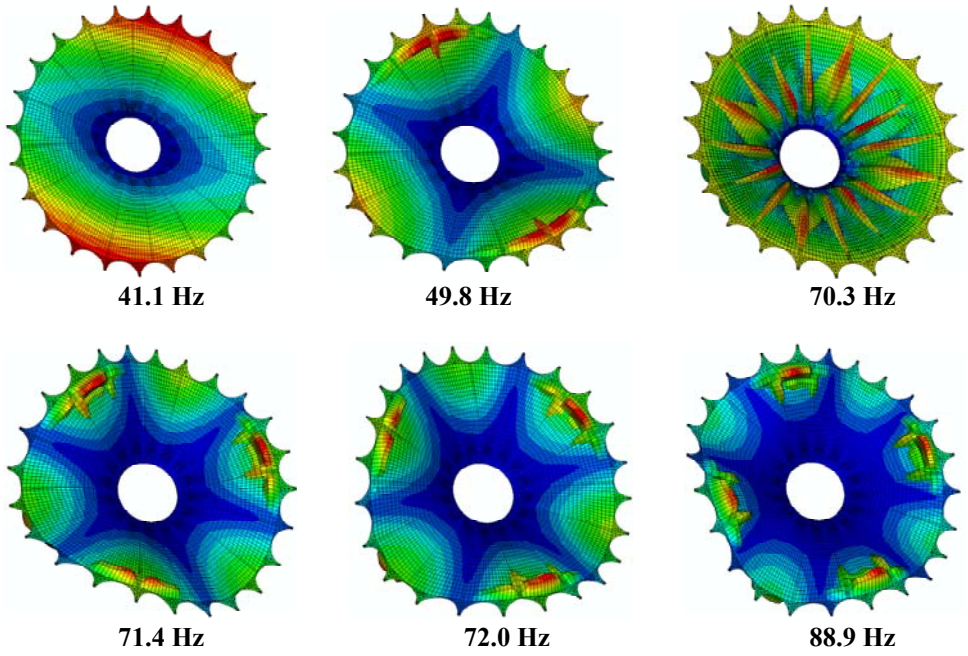

Figure 20: Normal modes of the 2 meter half-scale inflatable antenna dish.

D. Dynamics Scaling of the 2 meter Antenna

While analyzing these antennas structural characteristics, a quick assessment of the applicability of dynamics scaling for the half-scale antenna was made in order to conduct a preliminary assessment of the feasibility of extrapolating responses of reduced-scale laboratory articles to predict responses of large scale antennas envisioned for space flight. Using the scaling recommendations in references 24-26, a quick analysis was performed to see the gross effect of the scaling of this 2 meter half-scale antenna to a 4 meter full scale antenna. The thickness of the membrane material, and material properties were kept same and only the geometric size of the antenna was increased to 4 meter diameter. The internal pressure was scaled down by a factor of 4, assuming that the internal pressure requirement is inversely proportional to square of the diameter. The Table I give a comparison of the surface deformation, and the natural frequencies of the two antennas. From the table it can be seen that the full scale antenna surface deformation, in terms of orders of magnitude, is not very different from that of the subscale antenna. However, the natural frequencies of the full scale antenna have gotten reduced by about a factor of 3, which is roughly about the square of the diameter.

Table 1: A comparison structural characteristics of the half-scale and full-scale antenna

Item	Half-Scale Antenna, 2 meter size	Full-scale Antenna, 4 meter size
Max. Deformation	1.3 mm	2.6 mm
Mode 1	41.06 Hz	16.17 Hz
Mode 2	49.80 Hz	17.07 Hz
Mode 3	71.38 Hz	25.71 Hz
Mode 4	72.00 Hz	25.84 Hz
Mode 5	70.30 Hz	32.53 Hz

V. Concluding Remarks

The practical application of nonlinear analysis methodologies to evaluate structural characteristics of ultra-thin membrane inflatable parabolic reflector antennas has been demonstrated. Many intricate details of the nonlinear analysis were described, and experiences, and insight gained were discussed. The nonlinear analysis of the ultra-thin membrane structure has been a challenging experience even with the use of most sophisticated structural analysis codes such as NASTRAN and ABAQUS, the studies showed approaches to the nonlinear solution, to overcome convergence problems, to speed up iterative solution, and to handle wrinkling of thin membranes in the antenna structural analysis. The static implicit analysis technique was found to be more accurate, and better suited for evaluating structural characteristics, although some convergence difficulties were encountered in certain loading conditions.

The salient structural characteristics of the 0.3meter subscale antenna, 2 meter half-scale antenna, and 4 meter full scale antenna were evaluated. The antenna reflector surface accuracies were presented in terms of maximum static deformation value for a reflector surface, as well as easily observable displacement fringe patterns on the surface. The structural dynamics characteristics of the reflector antenna were presented in terms of underlying structural frequencies and normal mode shape patterns. The deformation pattern of the 4x6 full scale model was seen to be significantly influenced by the steep curvature associated with its off-axis orientation of the surface, while such pattern was not so dominant in the 0.3 meter reduced scale model. It was seen that antenna reflector surface accuracies are very much dependent on the type and size of the antenna, the reflector surface curvature, reflector membrane supports in terms of the spacing of catenaries, as well as the amount of tension load applied, internal pressure, and gravity loads, and the amount of wrinkling present in the antenna membrane surface.

Wrinkling pattern results were presented for the 0.3 meter antenna, which showed how the wrinkles progressed as tension load was increased in steps. Alternate means for overcoming nonlinear solution convergence problems arising due to thin membrane wrinkle instabilities were discussed. Those alternatives included (1) dynamic implicit and explicit analysis on the statics problem by including inflation dynamics to overcome wrinkling instabilities in the solution, (2) wrinkle algorithm in the solution process, and (3) enforcing uniformity of tension load at catenary attachment points with the membrane to avoid wrinkling. Dynamic implicit analysis techniques posed less of a convergence problem, but it use necessitate a more careful assessment of static deformation from the applied dynamic loading.

While analyzing the antennas structural characteristics, a quick assessment of the applicability of the dynamical scaling of a 2 meter half-scale antenna was made to extrapolate for responses of a 4 meter full-scale antenna. It was found that although the static structural response of the full scale model was of same order of magnitude as that of the reduced scale model, the dynamics in terms of the natural frequencies were significantly different.

It has been shown that development of better analytical models of antenna structures along with application of varieties of solution techniques have improved reliability of numerical predictions of reflector surface characteristics. Numerical predictions are crucial, when laboratory simulations of lightly loaded and highly flexible antennas are difficult, or when large scale tests are not practical. These structural analysis results are first step toward realistic application of the nonlinear analysis methodology, and further analysis is needed to verify the surface accuracies, and the load carrying capabilities of such inflatable membrane antennas.

Acknowledgments

The work described in this paper was funded by the Antenna Technology Program, which is managed by NASA's Space Operations Mission Directorate in Washington, D.C., and implemented by the Antenna Technology Office at Glenn Research Center in Cleveland, Ohio.

References

1. Anderson, L.J., Groth, L.H., "Reflector Surface Deviations in Large Parabolic Antennas", IEEE Transaction on Antennas and Propagation, March , 1962.

2. Ruze, J., "Antenna Tolerance Theory – A Review", Proceedings of IEEE, Vol. 54. No.4, April, 1966.

3. Milliken, S.A., "The development of high-gain deployable antenna for communication satellites", AIAA 66-306, AIAA Communication Satellite System Conference, Washington D.C., May 1966.

4. Archer, J.S., "High Performance Parabolic Antenna Reflectors, J. of Spacecraft, Vol. 17, No. 1, 1978.

5. Rusch, W.V.T, "The current state of the reflector antenna art", IEEE Transactions on Antennas and Propagation, Vol. AP-32, No.4, April, 1984.

6. Card., M.F, Boyer, W.J., "Large Space Structures - Fantasies and Facts", AIAA paper 80-0674, AIAA Conference 1980.

7. Friese, G.J., Bilyeu, G.D., Thomas, M., "Initial '80s Development of Inflated Antennas, L'GARDE Inc, NASA contractor report 166060, Jan. 1983.

8. Campbell, T.G., Bailey, Belvin, K.W, "The development of the 15-meter hoop column deployable antenna system with structural and electromagnetic performance results", AIAA 86-0667, 1986

9. Reaves, M.C, Belvin, K.W, and Bailey, J.P., "Finite-Element-Analysis Model and Preliminary Ground Testing of Controls-Structures Interaction Evolutionary Model Reflector", NASA TM - 4293, May 1992.

10. Hedgepeth, J.M., "Critical Requirements for the Design of Large Space Structures, NASA Contractor report -3484, Nov, 1981

11. Benton, B, "Thermal Control of Large Spacecraft Antenna Reflectors", AIAA-84-1777, AIAA 19th Thermophysics Conference, Colorado, 1984

12. Hedgepeth, J.M, "Interaction Between An Inflated Lenticular Reflection and Its Rim Support", AIAA-95-1510-CP, AIAA conference, 1995.

13. Gaspar, J.L., Sreekantamurthy, T., Mann T., Behun, V., Romanofsky, R.R, Lambert, K, Pearson, J, "Test and Analysis of Inflatable Parabolic Dish Antenna", AIAA-2006-1600 paper, AIAA SDM conference, Newport, Rhode Island 2006.

14. Pearson, J.C., Romanofsky, R.R, "Thin Film Antenna Development and Optimization", AIAA-2006-2229, AIAA 47th SDM, April 2006.

15. Lester, D.M., Wassom, S.R, Pearson, J.C, Holmes, M.R., "Solar Thermal Propulsion IHPRPT Demonstration Program", AIAA-2000-5109, 2000.

16. Casiano, M.J, Hamidzadeh, H.R, Tinker, M.L., "Dynamics of a 4x6 meter Thin Film Elliptical Inflated Membrane for Space Applications", AIAA-2002-1557, AIAA 43rd SDM conference, April 2002.

17. Willey, C.E., Schulze, R.C, Bokulic, R.S., Skullney, W.E, "A Hybrid Inflatable Dish Antenna System for Spacecraft ", AIAA 2001-1258, AIAA 42nd SDM Conference, April 2001.

18. MSC/NASTRAN software, MSC Software Corporation, Santa Ana, CA 92707, http://www.mscsoftware.com/products/msc_nastran.cfm

19. ABAQUS software, ABAQUS,Inc. Providence, RI 02909–2499, http://www.abaqus.com

20. Stein, M, and Hedgepeth, J.M., "Analysis of Partly Wrinkled Membranes ", NASA TN D-813, July 1961.

21. Miller, R.K, and Hedgepeth, J.M., "An Algorithm for Finite Element Analysis of Partly Wrinkled Membranes", AIAA 82-4293, Dec., 1982.

22. Adler, A.L, Mikulas, M.M., Hedgepeth, J.M., "Static and Dynamic Analysis of Partially Wrinkled Membrane Structures", AIAA-2000-1810, AIAA 41st SDM conference, Atlanta, GA, 2000.

23. Adler, A.L., Finite Element Approaches For Static And Dynamic Analysis Of Partially Wrinkled Membrane Structures, Ph.D. Thesis, Department of Aerospace Engineering, University of Colorado, 2000.

24. Thomas, M., and Veal, G, "Scaling characteristics of inflatable paraboloid concentrators", ASME, Solar Engineering, Edited Book number, H00630, 1991.

25. Thomas, M., and Friese G. J., "Pressurized antennas for space radars". Sensor Systems for the 80's Conference, Colorado Springs, Cab, December 2-4, 1980, Technical Papers. (A81-13351 03-35) New York, AIAA Inc., 1980, p. 65-71.

26. Greschik, G, Mikulas, M.M., and Freeland, R. E., "The nodal concept of deployment and the scale model testing of its application to a membrane antenna", AIAA-99-1523

27. Gaspar, J.L., Mann T., Sreekantamurthy, T., Behun, V. "Structural Test and Analysis of a Hybrid Inflatable Antenna", AIAA-07-1832 paper, AIAA SDM conference, Honolulu, Hawaii, April 2007